

# A molecular physiology basis for functional diversity of hydrogen peroxide production amongst *Symbiodinium* spp. (Dinophyceae)

Samantha Goyen<sup>1</sup> · Mathieu Pernice<sup>1</sup>  · Milán Szabó<sup>1</sup> · Mark E. Warner<sup>2</sup> · Peter J. Ralph<sup>1</sup> · David J. Suggett<sup>1</sup>

Received: 2 August 2016 / Accepted: 9 January 2017 / Published online: 16 February 2017  
© Springer-Verlag Berlin Heidelberg 2017

**Abstract** Hydrogen peroxide (H<sub>2</sub>O<sub>2</sub>) production has been demonstrated to play a pivotal role in the photosynthetic stability of higher plants, corals and algae, and considered a primary reactive oxygen species (ROS) associated with the thermal susceptibility of *Symbiodinium* spp. Here, we simultaneously subjected a large number of *Symbiodinium* isolates ( $n=16$ ) covering broad phylogenetic diversity (clades A, B, D, F) to heat stress and characterized their photosynthetic response via fast repetition rate fluorometry (FRRf) and parallel measurements of H<sub>2</sub>O<sub>2</sub> emissions. Based on their physiological response, isolates clustered into three novel functional groups: (1) thermally tolerant (unchanged photochemical efficiency ( $F_v/F_m$ ), electron turnover ( $\tau_{QA}$ ) or H<sub>2</sub>O<sub>2</sub> emission), or (2) thermally susceptible via decreased  $F_v/F_m$ , unchanged  $\tau_{QA}$ , but increased H<sub>2</sub>O<sub>2</sub>, indicating energetically uncoupled PSII (thylakoid membrane instability), versus (3) thermally responsive via decreased  $F_v/F_m$ , increased  $\tau_{QA}$  and H<sub>2</sub>O<sub>2</sub>, indicative of energetically coupled (but downregulated) PSII. There was no correlation between the algal phylogenetic groups and the distribution of isolates amongst these novel functional

groups. Two model *Symbiodinium* isolates for functional groups (1) and (2) (ITS2 type A1, *Symbiodinium microadriaticum*, and type D1–5, *Symbiodinium* spp., respectively) were selected to further examine how their different thermal responses corresponded with the expression levels of two genes coding for different metalloforms of superoxide dismutase (MnSOD and NiSOD) that potentially regulate production of H<sub>2</sub>O<sub>2</sub>. *S. microadriaticum* demonstrated the greatest upregulation of MnSOD gene confirming recent suggestions of a role for this metalloform in the antioxidant network associated with thermal stress protection. Assigning *Symbiodinium* isolates into such functional groups based on coupled molecular-physiological assessment is an important step needed to improve our understanding of *Symbiodinium* diversity relative to its ecological success in nature.

## Introduction

Reef building corals sustain immensely productive and biologically diverse ecosystems via a unique symbiosis with dinoflagellate microalgae (genus *Symbiodinium*) housed within the cnidarian tissue. Corals harbour an astonishing diversity of *Symbiodinium* spp., which is divided into nine phylogenetic clades (A–I, Pochon and Gates 2010) that in turn comprise hundreds of genetically distinct types (e.g. LaJeunesse et al. 2012; Pochon et al. 2014; Arif et al. 2014). At relatively broad phylogenetic levels, *Symbiodinium* genetic diversity associates with physiological traits that may influence overall fitness of the coral-symbiont association, for example the capacity to harvest and utilize light energy (Suggett et al. 2015; Warner and Suggett 2016). However, it is increasingly recognized that functional diversity of such traits within *Symbiodinium*'s

Responsible Editor: L. D. Mydlarz.

Reviewed by T. C. LaJeunesse and an undisclosed expert.

**Electronic supplementary material** The online version of this article (doi:10.1007/s00227-017-3073-5) contains supplementary material, which is available to authorized users.

✉ Mathieu Pernice  
mathieu.pernice@uts.edu.au

<sup>1</sup> Climate Change Cluster, University of Technology Sydney, Ultimo, NSW 2007, Australia

<sup>2</sup> College of Earth, Ocean, and Environment, University of Delaware, Lewes, DE 19958, USA

complex phylogeny is likely a more robust correlate of coral fitness (Parkinson and Baums 2014; Warner and Suggett 2016).

Anomalous light and temperature exposure are integral factors that can destabilize the coral-dinoflagellate symbiosis (Lesser and Farrell 2004) to result in coral bleaching. One of the primary sites of light and thermal stress-induced bleaching is loss of integrity to *Symbiodinium*'s photosynthetic apparatus (Warner et al. 1999; Tchernov et al. 2004; Buxton et al. 2012), caused by and/or leading to excessive production of reactive oxygen species (ROS) (reviewed by Warner and Suggett 2016) including hydrogen peroxide ( $H_2O_2$ ) (Tchernov et al. 2004; Smith et al. 2005).  $H_2O_2$  production can occur via several pathways (Warner and Suggett 2016), notably activity of MAP (Mehler–Ascorbate Peroxidase) and photorespiration (Lesser 2006; Fahnstich et al. 2008) within the chloroplasts, as well as mitochondrial alternative oxidase (AOX) (Rhoads et al. 2006). All of these pathways effectively act as energetic sinks by consuming excess electron pressure, intracellular  $O_2$ , ATP and/or NADPH, with MAP particularly predominating for *Symbiodinium* cells when in culture (Roberty et al. 2014, 2015; but see also). Indeed, MAP-based production of  $H_2O_2$  has been specifically suggested as a key factor regulating sensitivity to thermal stress in *Symbiodinium* (Smith et al. 2005; Suggett et al. 2008; Krueger et al. 2014; Roberty et al. 2015) via an imbalance between  $H_2O_2$  produced by superoxide dismutase (SOD) and  $H_2O_2$  consumed by ascorbate peroxidase (APX). However, enhanced production of  $H_2O_2$  has been observed for both thermally sensitive (Suggett et al. 2008) and tolerant (Roberty et al. 2015) *Symbiodinium* phylotypes under heat stress, likely reflecting complexities in how these algae differentially regulate SOD (McGinty et al. 2012; Levin et al. 2016) or APX (Krueger et al. 2014) capacity, which in the latter case is further linked to glutathione redox homeostasis (Krueger et al. 2014; Roberty et al. 2015). Such dynamics become further complicated for *Symbiodinium* cells in hospite given additional capacity for the host to quench or produce  $H_2O_2$  (Smith et al. 2005; Armoza-Zvuloni and Shaked 2014).

In efforts to better resolve the complexities underpinning the (MAP-based) ROS anti-oxidant network, researchers have increasingly turned to molecular, and specifically transcriptional, profiling based analysis of *Symbiodinium* cultures (Leggat et al. 2007; Bayer et al. 2012; Ladner et al. 2012). Most recently, transcripts of anti-oxidant genes have been successfully amplified for *Symbiodinium* ITS2-types B1, E and F1 (e.g. MnSOD, FeSOD and KatG; Krueger et al. 2015a) and a type C1 (Cu/ZnSOD, MnSOD, FeSOD and NiSOD metalloforms; Levin et al. 2016), to yield evidence for upregulation of the entire anti-oxidant network, including various SOD metalloforms under thermal stress for a thermally tolerant type C1 isolate (Levin

et al. 2016). Whilst such studies represent an important step change in how regulation of the anti-oxidant network can be described and, therefore, understood the actual link between the transcriptional response (genes of interest) and the production of the ROS of interest is still missing.

Existing evidence for a broad range of responses in  $H_2O_2$  production and in expression of constituents of antioxidant networks is perhaps not surprising given *Symbiodinium*'s immense phylogenetic diversity, thereby enabling adaptation to very different environmental states (e.g. Hume et al. 2015); however, it is also likely that phylogenetic patterns in mechanisms underpinning stress tolerance have not been established since only a relatively small pool of genetic variants have ever been examined at any one time (see Warner and Suggett 2016). Larger scale taxonomic screening of key photosynthetic traits amongst *Symbiodinium* spp. ( $n=18$  genetic variants) recently revealed that “functional groups” can be identified that do not exclusively conform to phylogenetic groups (Suggett et al. 2015); however, how such functional groupings apply under thermal stress has not yet been tested. Indeed, Wietheger et al. (2015) recently demonstrated that *Symbiodinium* spp. photosynthetic performance does not always respond to thermal- and  $H_2O_2$ -stress in a consistent manner. However, it should be noted that their study utilised extremely high exogenous  $H_2O_2$  concentrations that presumably more closely reflect host generated (as opposed to *Symbiodinium* intracellular derived) processes (e.g. Krueger et al. 2015b). Even so, the various responses observed by Wietheger et al. (2015) provided evidence that a single  $H_2O_2$ -based model for thermal susceptibility (*sensu* Tchernov et al. 2004; Smith et al. 2005) unlikely applies across all genetic variants. Here, we build on these recent observations and revisit *Symbiodinium* spp. photochemical competency of photosystem II (PSII) (a key diagnostic of stress susceptibility; e.g. Warner and Suggett 2016) in parallel with  $H_2O_2$  production under heat stress across multiple ( $n=16$ ) genotypes; from this, we were able to define for the first time novel functional groups for thermal stress related  $H_2O_2$  production. Using two model genotypes from these groups (A1, *Symbiodinium microadriaticum*, versus *Symbiodinium* sp. D1–5) we further link genotype-specific differences in  $H_2O_2$  production with level of expression of genes coding for two different metalloforms of superoxide dismutase (MnSOD and NiSOD) in response to thermal stress.

## Methods

### *Symbiodinium* culturing and experimental design

Sixteen strains from the genus *Symbiodinium* spanning four phylogenetic clades (A, B, D, F) were grown at 25 °C under

a 12:12 light: dark cycle with a photon flux density (PFD) ( $4\pi$  LI-190SA Quantum Sensor, Licor) of ca.  $85 \mu\text{mol photons m}^{-2} \text{s}^{-1}$ . Thirteen of these strains have been previously classified at the intracladal scale by their rDNA internal transcribed spacer 2 regions (ITS2) (as per Robison and Warner 2006; LaJeunesse et al. 2012; Suggett et al. 2015), with several of these now formally classified as species (LaJeunesse et al. 2012, 2015; Lee et al. 2015); specifically, *S. microadriaticum* (A1, rt61), *S. tridacnidorum* (A3, A3c, CS159 and CCMP2465 respectively), *S. lincheaea* (A4, rt379), *S. necroappetens* (A13, rt80), *S. pseudominutum* (B1, rt12), *Symbiodinium* sp. (B1', UTSB), *S. psygmophilum* (B2, Mf14.10), *Symbiodinium* sp. (D1–5, PHMSTD4), *S. kawagutii* (F1, CS156 and UTSC) and *Symbiodinium* sp. (F2, rt133); two different strains for each of A3, B1 and F1 were grown and, therefore, will be referred to here as A3 (CS159) and A3' (CCMP2465), B1 (rt12) and B1' (UTSB), and F1 (CS156) and F1' (UTSC), respectively; it should be noted that these two B1 isolates have been designated two separate species but with UTSB not confirmed as *S. minutum* (see Suggett et al. 2015). Two D-clade strains ( $D_{S1}$ ,  $D_{S2}$ ) were also analysed, however, they were identified based on sequence divergence in the chloroplast 23S rDNA and not by ITS2. Full details of these strain identities and original isolation histories are reported in Suggett et al. (2015). An additional alga from clade A of unknown origin, based on the 28S rRNA sequence (99.8% similarity to GenBank accession number AF427455) (see Buxton et al. 2012), was also grown and is referred to here as strain 'A'. All cultures were maintained semi-continuously in IMK artificial seawater media (Daigo IMK, Nihon Pharmaceutical Co., Ltd.) in exponential growth phase and optically thin with mean growth rates of  $0.19\text{--}0.26 \text{ day}^{-1}$  over 8–10 sequential generations (see Suggett et al. 2015) and cell densities maintained under  $80 \times 10^4 \text{ cells mL}^{-1}$ .

To assess for physiological thermal stress responses and  $\text{H}_2\text{O}_2$  production, 60 mL aliquots from each culture under steady state growth were dispensed evenly across triplicate control and treatment vials. For the duration of the experiment, control vials were maintained within an incubator set to the same conditions used for growth (i.e.  $85 \mu\text{mol photons m}^{-2} \text{s}^{-1}$  on a 12:12 light:dark cycle,  $25^\circ\text{C}$ ). Treatment vials were maintained within an identical incubator and subjected to 72 h thermal ramping from  $25$  to  $32^\circ\text{C}$ , as per Robison and Warner (2006). All vials were maintained at  $32^\circ\text{C}$  for a further 72 h to, therefore, yield a total incubation time of 144 h. Samples were taken from all vials for photophysiological analysis and cell counts at 0, 72 and 144 h, and for  $\text{H}_2\text{O}_2$  production at 144 h only. All samples were taken at 09:00 to eliminate any variation due to the natural diel cycle of *Symbiodinium* in the measured physiological parameters and in accordance with incubator light cycles (12:12 cycle, 08:00 local time lights on) (e.g. Sorek

et al. 2013). Biomass consistently increased whilst photo-physiological parameters were not significantly different for the control vials across the three sampling time points (data not shown) indicating that this set up provided conditions that matched those from the initial steady state culture inoculum, and cultures did not run into nutrient starvation, for the duration of the experiment.

### Photophysiology, cell counts and $\text{H}_2\text{O}_2$ quantification

All samples were acclimated to extremely low light (ca.  $\sim 5 \mu\text{mol photons m}^{-2} \text{s}^{-1}$ ) for at least 20 min prior to photophysiology measurements. All samples were then analyzed using a *FastOcean* Fast Repetition Rate fluorometer (FRRf) coupled to a *FastAct* base unit (Chelsea Technologies Group, UK). Excitation was delivered using a blue LED excitation source (peak excitation 450 nm) delivering an ST induction protocol of 100 flashlets of  $1.1 \mu\text{s}$  at  $2.8 \mu\text{s}$  (see Suggett et al. 2015). The FRRf was programmed to record the average of 40 sequential ST acquisitions at 150 ms intervals. Photosystem II (PSII) photophysiological characteristics were then determined by fitting acquisitions to the KPF model (Kolber et al. 1998) using FastPRO software (Chelsea Technologies Group, UK) to yield the minimum ( $F_o$ ) and maximum ( $F_m$ ) PSII fluorescence yields (instrument units), PSII absorption cross section ( $\sigma_{\text{PSII}}$ ;  $\text{nm}^2$ ), and the  $Q_A$  reoxidation rate ( $\tau_{Q_A}$ ,  $\mu\text{s}$ ). Cell counts were taken for each sample after FRRf analysis using a haemocytometer as per Hennige et al. (2009). All fluorescence yields were adjusted for baseline fluorescence using sample filtrate (see Suggett et al. 2015).

An Amplex Red-based assay was used to quantify hydrogen peroxide ( $\text{H}_2\text{O}_2$ ) using the protocol provided (Invitrogen, Molecular Probes<sup>®</sup>) and following modifications for *Symbiodinium* (Suggett et al. 2008; see also; Roberty et al. 2015). Amplex red reagent was added to the final reaction mixture made up of a 0.25 M sodium phosphate buffer, pH 7.4,  $0.1 \text{ U mL}^{-1}$  HRP and combined with 1 mL aliquots of sample and no  $\text{H}_2\text{O}_2$  controls. Samples were incubated for 1 h at their respective control or treatment temperatures, and under a Rose Pink screening filter (002, Lee Filters, Sydney, Australia) delivering a high PFD of  $700 \mu\text{mol photons m}^{-2} \text{s}^{-1}$  (Cidly Phantom 300W, Shenzhen, China) to maximize the  $\text{H}_2\text{O}_2$  signal:noise under light saturation (as per Suggett et al. 2008). The Rose Pink filter was placed over the incubation chamber in between the light source and samples to avoid reactions due to blue–green light,  $\sim 450$  to  $550 \text{ nm}$ . Following incubation, samples were centrifuged to pellet the cells and read using a spectrophotometer (Agilent Cary 60 UV–Vis, USA) at  $571 \text{ nm}$  against a reference blank (distilled water). Concentrations of  $\text{H}_2\text{O}_2$  were calculated using the absorbance values of the unknown samples compared to a series of standards of known  $\text{H}_2\text{O}_2$

concentrations (0–20  $\mu\text{M}$ ) containing the Amplex Red mixture, which were used to create a standard curve. All measures of  $\text{H}_2\text{O}_2$  concentration were normalised to corresponding measures of cell concentration for each sample; whilst we report our data throughout as  $\text{pmol H}_2\text{O}_2 \text{ cell}^{-1}$  (as per Suggett et al. 2008), values strictly reflect the  $\text{H}_2\text{O}_2$  emitted per cell per hour incubation.

### Gene expression

From the 16 *Symbiodinium* strains initially analysed for physiological characteristics and  $\text{H}_2\text{O}_2$  production, two strains, *S. microadriaticum* (A1, rt61) and *Symbiodinium* sp. (D1–5, PHMSTD4), were subsequently selected for expression analysis of two target genes coding for metalloforms of superoxide dismutase (MnSOD and NiSOD) and three reference genes (GADPH, Rp-S4 and psbA). These two target genes were chosen as these metalloforms were the only conserved regions found amongst the types tested. Both strains were again assayed using the exact same heat stress and control procedures as before but with increased replication ( $n=4$ ) and volume (100 mL per replicate); the % change for all photophysiological parameters and for  $\text{H}_2\text{O}_2$  production between control and treatment was not statistically different for this second repeat versus initial assay ( $t$  test; not shown) for either strain. All control and treatment replicates were processed as follows:

1. RNA extraction: an aliquot of 40 mL ( $\sim 10^{6-7}$  cells) was used for the RNA extraction where samples were centrifuged (10 min at  $2300\times g$ ) and the resulting cell pellets were snap-frozen in liquid nitrogen and stored at  $-80^\circ\text{C}$  until analysis (McGinley et al. 2012; Rosic et al. 2011). Total RNA was extracted using a Qiagen RNeasy Mini Kit (Qiagen, Australia). Cell pellets were first homogenized using a bead beater (Biospec, USA) and  $\sim 0.2$  g of 425–600 microns glass beads with the following cycle: agitation for 25 s at 30 1/s followed by a 5 s interval and a further 25 s at 30 1/s. Samples were then centrifuged for 10 min at  $16,000\times g$ . The aqueous phase was then used for RNA extraction using Qiagen RNeasy Mini Kit (Qiagen, Australia) according to manufacturer's instructions. RNA yield and purity was checked for each sample using a Nanodrop (Thermo Scientific, USA).
2. cDNA synthesis: a total of 100 ng of total RNA was used for cDNA synthesis for each sample, using the High-Capacity cDNA Reverse Transcription Kit (Applied Biosystems®) according to manufacturer's instructions. Briefly, a master mix containing  $10\times$  RT buffer,  $25\times$  dNTP Mix (100 mM),  $10\times$  RT Random Primers, Multiscribe Reverse Transcriptase, nuclease-

free water and 100 ng of total RNA was added to PCR tubes. PCR was conducted using a Veriti® 96-Well Thermal Cycler, Applied Biosystems® machine with cycling conditions as follows: initial denaturation step at  $25^\circ\text{C}$  for 10 min followed by denaturation at  $37^\circ\text{C}$  for 120 min, annealing at  $85^\circ\text{C}$  for 5 min and extension at  $4^\circ\text{C}$ . RT random primers were used to initiate cDNA synthesis. A DNase step was included to remove contaminating genomic DNA according to manufacturer's instructions. The cDNA was then diluted 1:50 with nuclease free water and used as the template (i.e. same cDNA quantity used for all samples) in the RT-qPCR analysis. No template control (NTC) and no reverse transcription controls (NRTC) were included for all gene/sample combinations to ensure that the cDNA samples were free of DNA contamination. All reactions were performed in triplicate, creating three technical replicates for each biological replicate (four biological replicates per treatment per strain).

3. Primer design and analysis: Target primers, amplifying 100–200 bp PCR products, were designed using Primer3 software based on sequence alignments from multiple *Symbiodinium* types obtained from the National Centre for Biotechnology Information (NCBI) GenBank database (<http://www.ncbi.nlm.nih.gov>); all other primers were sourced from the literature and validated using NCBI Basic Local Alignment Search Tool (BLAST) (<http://blast.ncbi.nlm.nih.gov/Blast.cgi>) (see Table 1). Standard PCR amplification was conducted for all primers to confirm the reproducibility and specificity of the primers for *Symbiodinium microadriaticum* and *Symbiodinium* sp. (D1–5). PCR conditions were as follows:

An initial denaturing step of 1 cycle at  $95^\circ\text{C}$  for 10 min, followed by 40 cycles of a denaturing step at  $95^\circ\text{C}$  for 30 s, an annealing step at  $60^\circ\text{C}$  for 30 s, and elongation at  $75^\circ\text{C}$  for 30 s. Samples underwent a final elongation step at  $72^\circ\text{C}$  for 5 min and then were held at  $10^\circ\text{C}$ . PCR products for all reference genes and genes of interest were visualized after gel electrophoresis (E-Gel® Imager System, Life Technologies, Australia), and sent to the Australian Genome Research Facility (AGRF) for sequencing to confirm primer specificity and sequence identity (Supplementary section Figs. 2 and 3). Primers were further quality controlled with amplification efficiency tests using RT-qPCR (StepOnePlus™ System, Applied Biosystems®) and the creation of a dilution curve using a threefold dilution series to cover a 80-fold range of concentrations (dilution 1:3, 1:9, 1:27, 1:81) and melt curve analysis. Three technical replicates for each cDNA

**Table 1** Primer sequences, amplicon length, melting temperature and literature source of the primers used as reference genes and genes of interest

Symbol	Forward primer sequence (5′–3′)	T <sub>m</sub> (°C)	Reverse primer sequence (5′–3′)	T <sub>m</sub> (°C)	Amplicon length (bp)	References
GAPDH	GGTGGTTGATGGCCAGAAGAT	60	CACCAGTGGATTTCGCAAACA	59	100	Rosic et al. 2011
Rp-S4	CCGCACAAACTGCGTGAGT	59	CGCTGCATGACGATCATCTT	58	101	Rosic et al. 2011
psbA	GAGTAGCTGGAGTATTTGGTG GAT	60	TGAAGGCTACGAGAGTTATTG AAG	58		McGinley et al. 2012
MnSOD	TCAACAAGAGGAGGCTGCTT	60	GACCTCCCTGACCTTCCCTA	60	149	This study
NiSOD	GAAGACTGCTTGGCCTTCAT	60	GACGACCACAGCCGACTACT	60	129	This study

The final column indicates studies of previously published sequences and those novel to this study

concentration were performed for each primer. For each primer set, technical triplicates were also included for a no template control (NTC) and a noRT control (NRTC) to ensure that the cDNA samples were free of DNA contamination. RT-qPCR settings were as follows: initial step at 95 °C for 30 s, cycling stage of 95 °C for 30 s, 60 °C for 30 s and 68 °C for 30 s, all for 50 cycles, melt curve stage of 95 °C for 15 s and 60 °C for 1 min and 95 °C for 15 s. Sample CTs were within the range of tested standard curves for all primers. All primers achieved efficiencies of 90–110% and were subsequently used in gene expression analysis.

4. Gene expression analysis: RT-qPCR assays were conducted for both strains using control and stress treatment cDNA with three technical replicates and four biological replicates. A master mix including diluted primers (final concentration 500 nM), ultra-pure water and SYBR Green PCR Master Mix (Applied Biosystems, including SYBR green as reporter dye) was made for each primer. 6 µL of each master mix and 4 µL of diluted cDNA (1:50 dilution) were loaded into each well of a 96 well standard microplate making a total reaction volume of 10 µL/well. Cycling conditions as above. Data from RT-qPCR was analysed using Step One Plus Software (Ver. 2.3; Applied Biosystems). Expression levels were determined as the number of cycles needed for the amplification to reach a fixed threshold in the exponential phase of the RT-qPCR reaction (Walker 2002). The cycle threshold (CT) was set at 0.03 for all genes. Replicate variability of the CT values between the three technical replicates, which were run on the same plate, was examined for each sample-gene combination. Repeatability of the assay between the technical replicates was consistent across the different genes with the replicate variability falling within the set limit of <0.5 cycles for all the

sample-gene combinations tested. To validate changes in target genes expression, CT were imported into the qbase + software package (Biogazelle).

### Statistical analysis

Independent *t* tests (MATLAB™) were used to compare FRRf-derived physiological parameters ( $F_v/F_m$ , dimensionless;  $\sigma_{PSII}$ , nm<sup>2</sup>;  $t_{QA}$ , µs) and H<sub>2</sub>O<sub>2</sub> concentration of replicate data ( $n=3$ ) for each strain between treatments (see supplementary section). Pairwise correlation and Bartlett's three-group model II linear regression with a least squares fit (MATLAB™) was used to compare for the general effect of heat treatment compared to control across all strains. Primer+Permanova (ver. 6.1; UK) was used to conduct multivariate analysis of physiological parameters (% change  $F_v/F_m$  and  $t_{QA}$ ) and % change H<sub>2</sub>O<sub>2</sub> concentration amongst strains using a Euclidian distance clustering and multidimensional scaling (MDS) to identify functional groups. A single % change value for each strain was calculated using the equation % change =  $([\bar{x}_t - \bar{x}_c]/\bar{x}_c) \times 100$ , where  $\bar{x}$  represents the mean from the three independent replicates for treatment (*t*) or control (*c*), and arcsine transformed and standardized prior to MDS analysis. For RT-qPCR data, the expression level of each target gene (MnSOD or NiSOD) was first normalized against the combination of three internal reference genes (Rp-S4, GAPDH and psbA, Table 1) using GeNorm algorithm (Hellemans et al. 2007) in order to obtain Normalized Relative Quantity for each treatment, which was then compared across treatment using an independent *t* test (SPSS Statistics Student Version 19 statistics program, Chicago, IL). The three internal reference genes used had a *M* stability (*M*) value under 1, reflecting a relative stability in gene expression. The data followed the linear model assumptions of independence, normality (Shapiro–Wilk test) and homoscedasticity (Levene's homogeneity test).

## Results

### Photophysiological and H<sub>2</sub>O<sub>2</sub> responses

FRRf-measurements under steady state growth conditions confirmed broad variation of both the PSII maximum photochemical efficiency ( $F_v/F_m$ , dimensionless) and effective absorption cross section ( $\sigma$ , nm<sup>2</sup>) across all 16 strains, ranging 0.39–0.48 and 3.7–5.3, respectively (Supplementary section; Fig. 1); values for both  $F_v/F_m$  and  $\sigma_{\text{PSII}}$  were generally within the range expected (Hennige et al. 2009; Suggett et al. 2015) and were negatively correlated (Fig. 1a) reflecting strain-specific differences in light harvesting efficiency (see Suggett et al. 2015). Subjecting the cells to heat stress, i.e. 72 h thermal ramping and subsequent exposure to 32 °C for a further 72 h, consistently decreased  $F_v/F_m$  (by 2–61%) and increased  $\sigma_{\text{PSII}}$  (by 0–63%) across all strains (except A4, D, and F2 where  $\sigma$  was decreased by 3–27%).

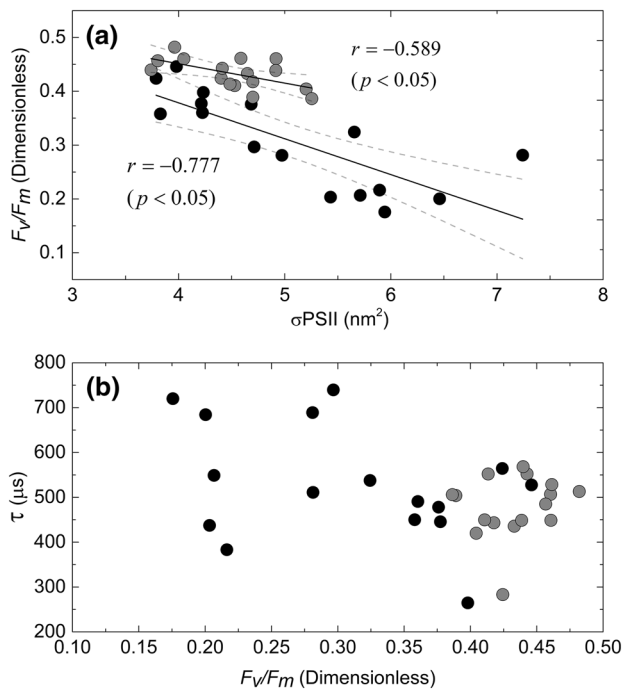


**Fig. 1** Relationship between corresponding FRRf-based measurements of **a** maximum PSII photochemical efficiency ( $F_v/F_m$ , dimensionless) and the PSII effective absorption cross-section ( $\sigma_{\text{PSII}}$ , nm<sup>2</sup>), **b**  $F_v/F_m$  and the  $Q_A$  re-oxidation rate ( $\tau_{\text{QA}}$ ,  $\mu\text{s}$ ). Data shown are for control (25 °C, grey circles) and heat treatment (32 °C, black circles), and with each circle representing the mean of replicate measurements ( $n=3$ ) for each *Symbiodinium* type ( $n=16$ ; see main text). Error bars are not shown for clarity (but see supplementary Table 1). Statistically significant correlations between corresponding measurements were only observed for **a**; the solid and dashed lines represent the linear relationship ( $\pm 95\%$  confidence limits) described by the equation  $F_v/F_m = (-0.036 \times \sigma_{\text{PSII}}) + 0.5954$  and  $F_v/F_m = (-0.067 \times \sigma_{\text{PSII}}) + 0.6451$  for 25 °C and 32 °C data, respectively. Control  $r^2 = 0.299$ ; treatment  $r^2 = 0.577$

This general parallel decline of  $F_v/F_m$  and increase of  $\sigma_{\text{PSII}}$  is indicative of a loss of PSII reaction center functionality in *Symbiodinium* spp. (Suggett et al. 2008; Ragni et al. 2010); however, the slope of the linear regression equation describing the covariance between  $F_v/F_m$  and  $\sigma$  was lower for the control versus heat stress ( $-0.036$  versus  $-0.067$ ) described by the equations:  $F_v/F_m = (-0.036 \times \sigma_{\text{PSII}}) + 0.5954$  and  $F_v/F_m = (-0.067 \times \sigma_{\text{PSII}}) + 0.6451$  for 25 °C and 32 °C data, respectively, (Fig. 1) and indicated a generally larger impact of heat stress on  $F_v/F_m$  than on  $\sigma_{\text{PSII}}$  across strains.

We further compared values of  $F_v/F_m$  with those of the  $Q_A$  re-oxidation rate ( $\tau_{\text{QA}}$ ,  $\mu\text{s}$ ) across all strains since two different trends for these parameters have previously been reported for *Symbiodinium* under heat stress; specifically, a reduction of  $\tau_{\text{QA}}$  with  $F_v/F_m$  indicative of a loss of thylakoid membrane integrity (Tchernov et al. 2004) and/or increased  $\tau_{\text{QA}}$  with decreased  $F_v/F_m$  indicative of a loss of PSII function (Robison and Warner 2006; Suggett et al. 2008). Under control temperatures  $\tau_{\text{QA}}$  values were highly variable across strains (280–570  $\mu\text{s}$ , see Supplementary section) and generally in the range previously reported (Tchernov et al. 2004; Suggett et al. 2008), but with no overall trend with corresponding values of  $F_v/F_m$  (Fig. 1b). Similarly, under heat stress values of  $\tau_{\text{QA}}$  were between 11% lower and 67% higher than the control values, and again with no trend with  $F_v/F_m$ . Thus, no consistent response for  $\tau_{\text{QA}}$  accompanied the generally reduced values of  $F_v/F_m$  across strains subjected to heat stress (Fig. 2b).

Cellular normalized H<sub>2</sub>O<sub>2</sub> release rates (pmol cell<sup>-1</sup>) under steady state ranged from 0.25 to 0.9 (*S. tridacnidorum* A3, A3c, *S. psygmophilum*, and *Symbiodinium* sp. D<sub>S2</sub> and F1) to 1.0–2.64 (all other strains) (Supplementary section) and hence no clear pattern with cladal identity; this range of H<sub>2</sub>O<sub>2</sub> concentrations was again consistent with values previously reported (Suggett et al. 2008; Roberty et al. 2015), and did not correlate with strain-specific differences in cell size (not shown). H<sub>2</sub>O<sub>2</sub> concentrations consistently increased under heat stress (by ca. 25–400%, Fig. 2a), and the % change in H<sub>2</sub>O<sub>2</sub> concentration between steady state control and heat stress treatment was generally (negatively) correlated with the corresponding % change in  $F_v/F_m$  as shown by the equation: % change H<sub>2</sub>O<sub>2</sub> =  $(-3.5475 \times \% \text{ change } F_v/F_m) + 79.405$  (Fig. 2a) but not % change in  $\tau_{\text{QA}}$  (not shown). Further MDS analysis across the 16 strains examining the corresponding % change for H<sub>2</sub>O<sub>2</sub>,  $F_v/F_m$ , and  $\tau_{\text{QA}}$ , further resolved the presence of three general ‘functional groups’ (Fig. 3):

1. Relatively unchanged  $F_v/F_m$ ,  $\tau_{\text{QA}}$ , i.e. thermally tolerant but with relatively (a) unchanged [*S. microadriaticum* (A1), *S. lincheaea* (A4), *S. necroappetens* (A13), *Symbiodinium* sp. D<sub>S2</sub>, and *S. kawagutii* (F1)] or (b)

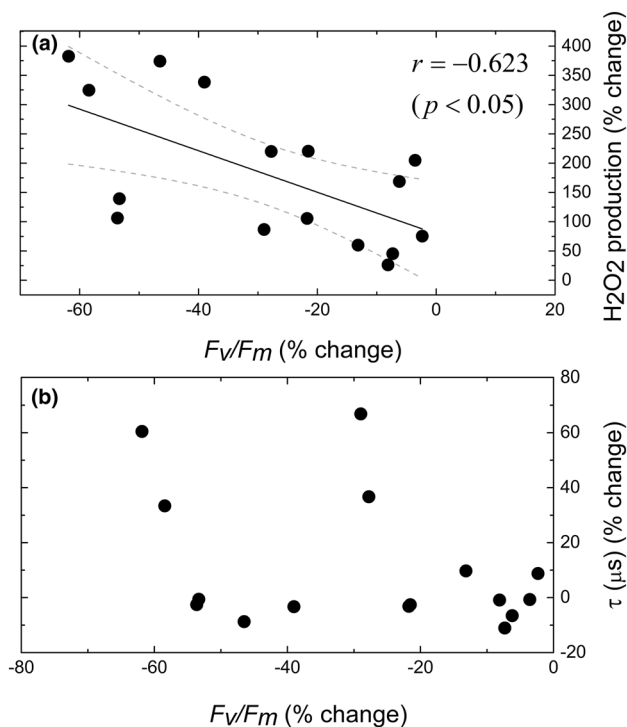


**Fig. 2** Relationship between **a** % change  $\text{H}_2\text{O}_2$  produced and % change  $F_v/F_m$  for heat stress relative to control samples (i.e. % change =  $([\text{Treatment} - \text{Control}]/\text{Control}) \times 100$ ), and **b** % change  $\tau_{QA}$  versus % change  $F_v/F_m$ . Each data point represents the % change calculated from the mean ( $n=3$ ) control and treatment value for each *Symbiodinium* type ( $n=16$ ; see main text). Statistically significant correlations between corresponding measurements were only observed for **a**; the solid and dashed lines represent the linear relationship ( $\pm 95\%$  confidence limits) described by the equation % change  $\text{H}_2\text{O}_2 = (-3.5475 \times \% \text{ change } F_v/F_m) + 79.405$ .  $r^2 = 0.344$

- enhanced (*Symbiodinium* sp. D<sub>S1</sub>, *S. kawagutii* (F1), and *Symbiodinium* sp. F2] emission of  $\text{H}_2\text{O}_2$ ;
2. Decreased  $F_v/F_m$ , unchanged  $\tau_{QA}$ , and increased  $\text{H}_2\text{O}_2$  [*S. tridacnidorum* (A3), *Symbiodinium* sp. B1', *S. psygmophilum* (B2), *Symbiodinium* sp. D1–5], consistent with patterns described by Tchernov et al. (2004) interpreted as thermal susceptibility via energetically uncoupled PSII, where the transmembrane proton gradient (established by the photochemical reactions in the functional reaction centers) is dissipated without generating ATP;
  3. Decreased  $F_v/F_m$ , increased  $\tau_{QA}$  and relatively (a) large [*Symbiodinium* sp. A, *S. tridacnidorum* (A3c), *S. pseudominutum* (B1)] or small (*S. tridacnidorum* (A3')) increases in  $\text{H}_2\text{O}_2$ , indicative of thermally responsive but via energetically coupled PSII, i.e. transmembrane proton gradient dissipation generates ATP;

Importantly, these three different functional groups do not cluster according to large phylogenetic groupings (i.e. clades), although only clades A and B fell within functional group (3).

### Molecular responses

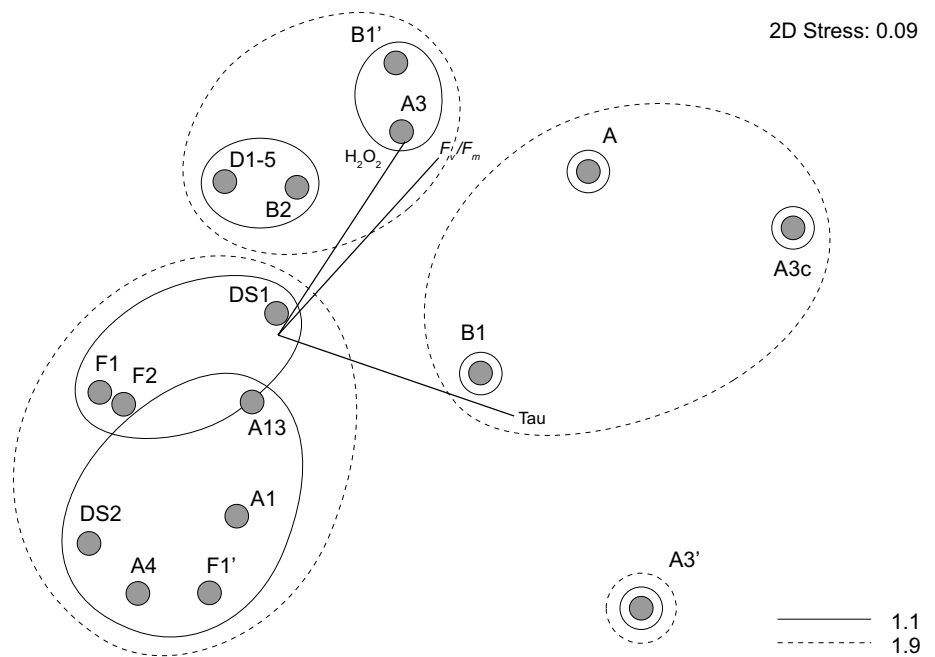
Whilst the number of *Symbiodinium* gene expression studies have increased substantially in the past decade, no universal primer set for reference genes are currently available which work across multiple *Symbiodinium* clades thereby limiting the application of RT-qPCR and the relative quantification method (Rosic et al. 2011). Thus, finding primers that successfully amplify reference genes appears problematic given the high level of sequence divergence between *Symbiodinium* clades. For our study, primers sets for the reference genes selected successfully amplified for both isolates of interest, *Symbiodinium* sp. (D1–5) and *S. microadriaticum* cDNA. Real-time dissociation curves further confirmed the presence of a specific PCR product in all amplification reactions.

RT-qPCR analysis revealed that heat stress significantly influenced the transcript abundance of *Symbiodinium* MnSOD; specifically, a ca. threefold increase in heat treated cells compared to the control for type A1 (Fig. 4) and a twofold increase for type D1–5 (Fig. 4). Whilst NiSOD expression also increased 1.4-fold under heat stress compared to control for type A1, this difference was not statistically significant (see Fig. 4 legend). Similarly, NiSOD was not significantly regulated for type D1–5 between heat stress and control. Overall the transcript abundance for both MnSOD and NiSOD for the A1 isolate ( $29.595 \pm 0.248$  and  $34.250 \pm 0.183$  Ct, respectively) was always higher than for D1–5 ( $28.505 \pm 0.141$  and  $32.895 \pm 0.290$  Ct, respectively) by ca. two orders of magnitude.

### Discussion

A major goal for the past two decades has been to identify how *Symbiodinium* spp. genetic variants respond to different stressors, in particular elevated temperature (e.g. Warner et al. 1996; Suggett et al. 2008; Takahashi et al. 2008; Buxton et al. 2012; McGinty et al. 2012; Krueger et al. 2014), to better understand how environmental variability influences ecological distribution (e.g. LaJeunesse et al. 2010, 2014) and physiological functioning (e.g. Warner et al. 2006) of these endosymbiont cells in nature. Elevated production of reactive oxygen species (ROS) appears a conspicuous feature of stress susceptibility amongst *Symbiodinium* genotypes (see Warner and Suggett 2016); however, both the form of ROS, and how (or if) it is produced amongst genotypes, appears highly variable

**Fig. 3** Functional groupings based on the physiological parameters associated with heat stress sensitivity (% change  $F_v/F_m$ ,  $\tau_{QA}$ ,  $H_2O_2$  concentration). Cluster analysis and multidimensional scaling (MDS) were performed on the average of each variable per variant (see the “Methods” section); similarity is shown at the 1.1 and 1.9 distance levels and vectors driving the clustering are shown in grey. Note only ITS2 type designation are shown for clarity and full detailed of isolates and taxonomic classification can be found in the material and methods



across studies examining relatively few isolates (e.g. Tchernov et al. 2004; Takahashi et al. 2008) thereby confounding efforts to reconcile observations and develop a general ROS-based paradigm of heat stress sensitivity. We, therefore, took the approach here of screening for a key ROS ( $H_2O_2$ , Smith et al. 2005) amongst numerous isolates covering four major clades (A, B, D, F) under heat stress to examine for potential phylogenetic patterns. Whilst patterns of photosynthetic physiology and  $H_2O_2$  emissions could not be reconciled with phylogenetic groupings, we uniquely observed two different functional responses to heat stress. Such a diversity of response is entirely consistent with the recent notion that a single model may be insufficient to explain patterns of heat stress susceptibility amongst the immense genetic diversity inherent to the genus *Symbiodinium* (Buxton et al. 2012; Warner and Suggett 2016).

Several prior studies have reported an increase in  $H_2O_2$  emission from heat stress sensitive *Symbiodinium* exposed to short-term temperature increases (clades A–C, Tchernov et al. 2004; ITS type B1; Suggett et al. 2008; Roberty et al. 2015). All of these observations correspond with parallel upregulation of light-dependent  $O_2$  consumption via photosystem I (notably Mehler Ascorbate Peroxidase activity, Roberty et al. 2016) presumably as excitation pressure as PSII goes into ‘over-drive’ (Lesser and Farrell 2004); however, our observations would in fact suggest that this general response manifests via two alternate modes of operation (at least according to the time scale with which strains were subject to heat stress here).

Our functional group (2) was consistent with photobiological trends reported by Tchernov et al. (2004), where

reduced/unchanged  $\tau_{QA}$  (alongside reduced  $F_v/F_m$ ) under heat stress was interpreted as  $H_2O_2$ -based lipid peroxidation resulting in higher excitation pressure through PSII; however, heat stress sensitivity was not consistent with phylogenetic groupings. A subsequent study by Hill et al. (2009) examining coral taxa hosting a range of ITS2 types from clades A, C and D similarly could not identify a link between sensitivity of thylakoid membrane stability under heat stress and phylogeny. In contrast, our functional grouping (3) reflected previous observations (Robison and Warner 2006; Suggett et al. 2008) of high-temperature destabilization of PSII via increased  $\tau_{QA}$ .

Fully reconciling the underlying reason for these different functional groups from this data is not possible. In part, the longer duration of heat stress (244 h) applied by Tchernov et al. (2004) may be required to overwhelm the physiological network that otherwise protects thylakoid stability. This process can clearly be short-circuited where the nature of heat stress is particularly acute relative to the upper thermal thresholds of any given isolate; for example, the relatively heat (32 °C) stress tolerant F1 (CS156) can exhibit a functional response (3) pattern when subjected to rapid acute heating (37 °C) (Hill et al. 2009). Some *Symbiodinium* types may in fact have an enhanced capacity for combatting lipid peroxidation (e.g. through volatile gas emissions, see Exton et al. 2015; anti-oxidant networks; Krueger et al. 2014) or are simply so leaky (reduced cell wall thickness) that contact time between  $H_2O_2$  and the lipid membranes is reduced (Wietheger et al. 2015); the latter process may perhaps also explain why some strains appear to show increased  $H_2O_2$  emission but no signs of



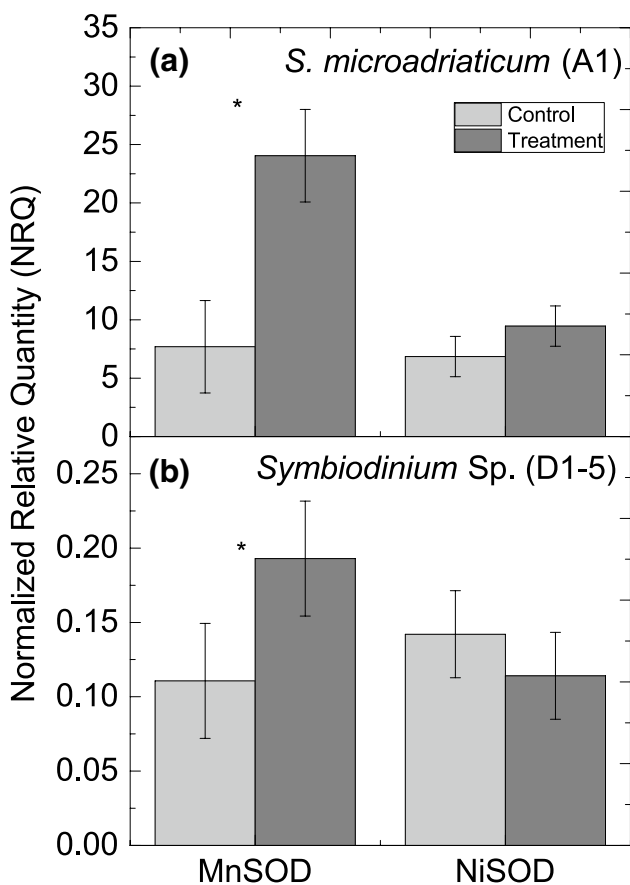


**Fig. 4** Mean  $\pm$  standard deviation ( $n=4$ ) of normalised relative quantity (NRQ) of the SOD genes (MnSOD and NiSOD) expression level for **a***S. microadriaticum* (A1) and **b***Symbiodinium* sp. (D1–5); both under control (25°C, light grey) and treatment (32°C, dark grey) temperatures. Relative quantity of MnSOD and NiSOD gene was normalised to the most stable reference genes as defined by GeNorm analysis (Rp-S4, GADPH and psbA) (see main text). NRQ was significantly different between control and treatment temperatures (independent  $t$  test) for MnSOD only, but for both ITS2 types A1 ( $p=0.038$ ) and D1–5 ( $p=0.047$ )

photophysiological sensitivity to heat stress [functional group (1b) (Wietheger et al. 2015)]. At present, the underlying reason is not entirely clear but regardless our observations of enhanced production of  $H_2O_2$  but different photobiological patterns is entirely consistent with the notion that *Symbiodinium* isolates do not express a universal response to heat stress (see Buxton et al. 2012; Warner and Suggett 2016).

On balance, our current observations from screening a substantial number of ITS2 types was able to resolve functional diversity that did not correspond with any pattern of phylogenetic diversity. Whether this lack of correspondence may in part reflect some of the challenges that remain in phylogenetically resolving *Symbiodinium* via ITS2 alone (e.g. Hume et al. 2015) versus convergent selection to localised ecological or environmental conditions (Parkinson

et al. 2015) from where the various isolates were originally sourced (see Suggett et al. 2015) is unclear. In the latter case, we observed a heat stress tolerant response for our *S. microadriaticum* isolate (A1) CCMP2464 (see also Suggett et al. 2008) that contrasts with a more heat sensitive response recently observed for a different *S. microadriaticum* species isolate (Mediterranean isolate “Avir”; Roberty et al. 2015). How heat stress exposure is conducted relative to differences in thermal history (e.g. isolates from different thermal regimes) is thus clearly important in defining differing physiologies and how isolates fall into their ‘functional groups’.

An important outcome of our study was subsequent targeted molecular evaluation of heat stress sensitivity. The two model strains selected appeared relatively thermally tolerant and susceptible, respectively, but both had low to moderate  $H_2O_2$  production (see “Results” section) and hence were likely to have differential molecular control of ROS anti-oxidants (e.g. Krueger et al. 2014, 2015a; Levin et al. 2016). Whilst these two strains did not cover all three emergent functional groups (above), i.e. only thermally tolerant [*S. microadriaticum*; group (1)] versus thermally susceptible via energetically uncoupled PSII [*Symbiodinium* sp. (D1–5); group (2)], they demonstrate clear differential heat stress sensitivity of SOD metalloform expression. *S. microadriaticum* exhibited greater SOD upregulation (and notably of MnSOD) over *Symbiodinium* sp. D1–5, suggesting that any additional SOD-based  $H_2O_2$  production be balanced through parallel upregulation of  $H_2O_2$  antioxidants; indeed, such a notion has recently been demonstrated for a thermally tolerant ITS2 type C1 isolate where upregulation of the entire anti-oxidant network occurred but no elevated ROS was observed under heat stress (Levin et al. 2016). Upregulation of genes (abundance and/or activity) involved in ROS scavenging is well established for *Symbiodinium* isolates under heat stress (e.g. Bayer et al. 2012; McGinty et al. 2012; Krueger et al. 2014). Light-activated ROS production may reflect elevated MAP activity to produce  $H_2O_2$  in the chloroplast (Suggett et al. 2008; Roberty et al. 2014); although how much  $H_2O_2$  produced is ultimately a function of ascorbate peroxidase activity and how it is coupled to the glutathione pathway, which are also potential variables amongst isolates (see Krueger et al. 2014).

Our observations overall would suggest a strong role for SOD metalloform MnSOD in heat stress tolerance of our isolates; however, Levin et al. (2016) demonstrate the importance of FeSOD in a thermally tolerant ITS2 type C1 isolate. Increased expression of MnSOD in response to heat stress has been generally well observed for coral hosts of *Symbiodinium* (e.g. Császár et al. 2009) but also *Symbiodinium* (Downs et al. 2013), and reflects upregulation of mitochondrial SOD in eukaryotes. Such a response is entirely consistent with the potential for mitochondria to

be significant sources of ROS (Lesser 2006; Warner and Suggett 2016), where mitochondria are also potential targets of heat stress within the host cnidarian (Dunn et al. 2012). Mitochondrial respiration occurs in *Symbiodinium* through the cytochrome c oxidase, Complex IV (COX) or the alternative oxidase enzyme (AOX) pathways, both enabling the reduction of O<sub>2</sub> to H<sub>2</sub>O via the oxidation of reduced cytochrome c (cytc) or of ubiquinone, respectively, (Oakley et al. 2014; Warner and Suggett 2016). The upregulation of MnSOD observed here could, therefore, point to thermal induced activation of the COX or AOX pathways. Both dark and light-enhanced (oxygen uptake in the light) respiratory rates are relatively high in *Symbiodinium* (Brading et al. 2011; Roberty et al. 2014). Likewise, some (Oakley et al. 2014) but not all (Roberty et al. 2015) studies clearly highlight upregulation of AOX as a mechanism contributing to the light-dependent O<sub>2</sub> consumption, leading to direct H<sub>2</sub>O<sub>2</sub> production. Whilst a role for mitochondrial based SOD upregulation is intriguing here, it is important to highlight two critical points at this stage.

First, MnSOD can be assigned to either secretory or mitochondrial pathways (Krueger et al. 2015a). Some *Symbiodinium* strains seem to lack or do not express FeSOD at all (Krueger et al. 2015a; Levin et al. 2016) suggesting that another SOD metalloform may in fact perform the role of FeSOD in the chloroplast. Other free-living microalgae, including cyanobacteria and diatoms, have an evolved localization of MnSOD in their chloroplasts (see Grace 1990; Wolfe-Simon et al. 2006), most likely to overcome Fe limitation and lower cellular Fe quotas. However, Fe requirements of *Symbiodinium* in culture, at least for *S. kawagutii* (Type F1), has recently been shown to be relatively large (especially compared to Mn and Ni) (Rodriguez et al. 2016) suggesting that FeSOD would be unlikely selected against unless *Symbiodinium* persisted in low Fe environments. Alternatively, MnSOD may be located in peroxisomes (see Lin et al. 2015 for *S. kawagutii*) and function well as a quencher of highly diffusible H<sub>2</sub>O<sub>2</sub>. In higher plants, peroxisomes generate superoxide and nitric oxide radicals (Schrader and Fahimi 2006) and thus also contain many antioxidant enzymes such as SOD and components of the ascorbate–glutathione cycle. Evaluating any upregulation of SODs specifically within the peroxisomes would, therefore, clearly enhance our current understanding of H<sub>2</sub>O<sub>2</sub> production within *Symbiodinium*.

Second, because sequences for MnSOD and FeSOD are very similar, having diverged from a common ancestor (Miller 2012), it is important to recognize that our RT-qPCR assay could have detected both metalloforms, and thus our observations do not necessarily preclude a lack of FeSOD in the strains tested. We have only focused on MnSOD and NiSOD here since these metalloforms were the only conserved regions found amongst the types tested;

however, further studies clearly need to consider the transcriptional regulation of other metalloforms, such as Fe, Cu and Zn as well as ROS enzymes (or proteins), considering also that dinoflagellates express a high degree of post-translational gene regulation where actual protein amount/activity might not be entirely represented through gene expression studies (Mayfield et al. 2014).

Few studies have yet undertaken a molecular physiology based approach to link genotype-specific differences in ROS production with transcriptional responses of the ROS network under thermal stress (e.g. Levin et al. 2016). However, here we have shown for the first time that production of a key specific ROS (H<sub>2</sub>O<sub>2</sub>) appears to correspond with differences in key ROS anti-oxidants/promoters, i.e. SOD that quenches superoxide to produce H<sub>2</sub>O<sub>2</sub>, amongst *Symbiodinium* isolates. Fully establishing the link between these two processes is not currently possible and reinforces recent suggestions that fully characterizing mechanisms of heat stress sensitivity ultimately require a complete picture of the physiological (Krueger et al. 2014; Warner and Suggett 2016) and/or molecular (Levin et al. 2016) network at play. Even so, this work demonstrates how heat stress sensitivity amongst *Symbiodinium* isolates, at least according to the parameters we have examined, can be ascribed to at least three functional groups, (1) tolerant, and sensitive as (2) energetically uncoupled versus (3) coupled PSII. Thus, heat stress sensitivity for *Symbiodinium* cannot be explained by a universal mechanistic description.

How *Symbiodinium* isolates fall into functional groups under heat stress sensitivity here does not appear to be the same as under steady state light utilization (Suggett et al. 2015); however, the traits examined in this study differ from those of Suggett et al. (2015), and thus, perhaps unsurprisingly, the choice of traits(s) will inevitably be an important consideration governing how taxa functionally group together. *Symbiodinium* have clearly evolved a wide range of mechanisms to tolerate heat stress (reviewed by Warner and Suggett 2016); consequently, studies attempting to better reconcile ecological patterns of *Symbiodinium* species diversity with temperature changes over space and time may ultimately need to consider a much broader range of diagnostic traits to temperature sensitivity to best describe functional diversity. Further, given the symbiotic nature of *Symbiodinium*, future studies examining this broader array of traits *in hospite* is clearly needed to confirm if *Symbiodinium* physiological responses and functional grouping observed in culture are still valid when compared to an intact symbiosis.

**Acknowledgements** The authors wish to thank two anonymous reviewers whose critical insight further improved this manuscript. In addition, to Paul Brooks and Lucia Mesarosova for technical support with *Symbiodinium* culturing and also Victor Beltran (Symbiont Culture Facility, Australian Institute of Marine Science, Townsville, Qld.,

Australia) for supplying strain amur-D-MI originally collected under permit G10-33440.1. DJS was funded by Australian Research Council (ARC) Future Fellowship FT130100202. The authors are particularly grateful to Ms. Rachel Levin, whose insightful comments on an earlier draft improved this MS.

## References

- Arif C, Daniels C, Bayer T, Banguera-Hinestroza E, Barbrook A, Howe CJ, LaJeunesse TC, Voolstra CR (2014) Assessing Symbiodinium diversity in scleractinian corals via next-generation sequencing-based genotyping of the ITS2 rDNA region. *Mol Ecol* 23:4418–4433
- Armoza-Zvuloni R, Shaked Y (2014) Release of hydrogen peroxide and antioxidants by the coral *Stylophora pistillata* to its external milieu. *Biogeosciences* 11:4587–4598
- Bayer T, Aranda M, Sunagawa S, Yum LK, DeSalvo MK, Lindquist E, Coffroth MA, Voolstra CR, Medina M (2012) Symbiodinium transcriptomes: genome insights into the dinoflagellate symbionts of reef-building corals. *PLoS One* 7:e35269
- Brading P, Warner ME, Davey P, Smith DJ, Achterberg EP, Suggett DJ (2011) Differential effects of ocean acidification on growth and photosynthesis among phylotypes of Symbiodinium (Dinophyceae). *Limnol Oceanogr* 56:927–938
- Buxton L, Takahashi S, Hill R, Ralph PJ (2012) Variability in the primary site of photosynthetic damage in *Symbiodinium* sp.(dinophyceae) exposed to thermal stress. *J Phycol* 48:117–126
- Császár NBM, Seneca FO, Van Oppen MJH (2009) Variation in antioxidant gene expression in the scleractinian coral *Acropora millepora* under laboratory thermal stress. *Mar Ecol Prog Ser* 392:93–102
- Downs CA, McDougall KE, Woodley CM, Fauth JE, Richmond RH, Kushmaro A, Gibb SW, Loya Y, Ostrander GK, Kramarsky-Winter E (2013) Heat-stress and light-stress induce different cellular pathologies in the symbiotic dinoflagellate during coral bleaching. *PLoS One* 8:e77173
- Dunn SR, Pernice M, Green K, Hoegh-Guldberg O, Dove SG (2012) Thermal stress promotes host mitochondrial degradation in symbiotic cnidarians: are the batteries of the reef going to run out? *PLoS One* 7:e39024
- Exton DA, McGenity TJ, Steinke M, Smith DJ, Suggett DJ (2015) Uncovering the volatile nature of tropical coastal marine ecosystems in a changing world. *Glob Change Biol* 21:1383–1394
- Fahnenstich H, Scarpeci TE, Valle EM, Flügge UI, Maurino VG (2008) Generation of hydrogen peroxide in chloroplasts of *Arabidopsis* overexpressing glycolate oxidase as an inducible system to study oxidative stress. *Plant Physiol* 148:719–729
- Grace SC (1990) Phylogenetic distribution of superoxide dismutase supports an endosymbiotic origin for chloroplasts and mitochondria. *Life Sci* 47:1875–1886
- Hellemans J, Mortier G, De Paeppe A, Speleman F, Vandesompele J (2007) qBase relative quantification framework and software for management and automated analysis of real-time quantitative PCR data. *Genom Biol* 8:R19
- Hennige SJ, Suggett DJ, Warner ME, McDougall KE, Smith DJ (2009) Photobiology of Symbiodinium revisited: bio-physical and bio-optical signatures. *Coral Reefs* 28:179–195
- Hill R, Ulstrup KE, Ralph PJ (2009) Temperature induced changes in thylakoid membrane thermostability of cultured, freshly isolated, and expelled zooxanthellae from scleractinian corals. *Bull Mar Sci* 85:223–244
- Hume BC, D'Angelo C, Smith EG, Stevens JR, Burt J, Wiedenmann J (2015) *Symbiodinium thermophilum* sp. nov., a thermotolerant symbiotic alga prevalent in corals of the world's hottest sea, the Persian/Arabian Gulf. *Sci Rep* 5:8562
- Kolber ZS, Prášil O, Falkowski PG (1998) Measurements of variable chlorophyll fluorescence using fast repetition rate techniques: defining methodology and experimental protocols. *BBA Bioenerget* 1367:88–106
- Krueger T, Becker S, Pontasch S, Dove S, Hoegh-Guldberg O, Leggat W, Fisher PL, Davy SK (2014) Antioxidant plasticity and thermal sensitivity in four types of *Symbiodinium* sp. *J Phycol* 50:1035–1047
- Krueger T, Fisher PL, Becker S, Pontasch S, Dove S, Hoegh-Guldberg O, Leggat W, Davy SK (2015a) Transcriptomic characterization of the enzymatic antioxidants FeSOD, MnSOD, APX and KatG in the dinoflagellate genus *Symbiodinium*. *BMC Evol Biol* 15:1
- Krueger T, Hawkins TD, Becker S, Pontasch S, Dove S, Hoegh-Guldberg O, Leggat W, Fisher PL, Davy SK (2015b) Differential coral bleaching—contrasting the activity and response of enzymatic antioxidants in symbiotic partners under thermal stress. *Comp Biochem Physiol A Mol Integr Physiol* 190:15–25
- Ladner JT, Barshis DJ, Palumbi SR (2012) Protein evolution in two co-occurring types of *Symbiodinium*: an exploration into the genetic basis of thermal tolerance in *Symbiodinium* clade D. *BMC Evol Biol* 12:1
- LaJeunesse TC (2005) “Species” radiations of symbiotic dinoflagellates in the Atlantic and Indo-Pacific since the Miocene-Pliocene transition. *Mol Biol Evol* 22:570–581
- LaJeunesse TC, Pettay DT, Sampayo EM, Phongsuwan N, Brown B, Obura DO, Hoegh-Guldberg O, Fitt WK (2010) Long-standing environmental conditions, geographic isolation and host-symbiont specificity influence the relative ecological dominance and genetic diversification of coral endosymbionts in the genus *Symbiodinium*. *J Biogeogr* 37:785–800
- LaJeunesse TC, Parkinson JE, Reimer JD (2012) A genetics-based description of *Symbiodinium minutum* sp. nov. and *S. psygmophilum* sp. nov.(Dinophyceae), two dinoflagellates symbiotic with cnidaria. *J Phycol* 48:1380–1391
- LaJeunesse TC, Wham DC, Pettay DT, Parkinson JE, Keshavmurthy S, Chen CA (2014) Ecologically differentiated stress-tolerant endosymbionts in the dinoflagellate genus *Symbiodinium* (Dinophyceae) Clade D are different species. *Phycologia* 53:305–319
- LaJeunesse TC, Lee SY, Gil-Agudelo DL, Knowlton N, Jeong HJ (2015) *Symbiodinium necroappetens* sp. nov. (Dinophyceae): an opportunist ‘zooxanthella’ found in bleached and diseased tissues of Caribbean reef corals. *Eur J Phycol* 50:223–238
- Lee SY, Jeong HJ, Kang NS, Jang TY, Jang SH, LaJeunesse TC (2015) *Symbiodinium tridacnidorum* sp. nov., a dinoflagellate common to Indo-Pacific giant clams, and a revised morphological description of *Symbiodinium microadriaticum* Freudenthal, emended Trench & Blank. *Eur. J Phycol* 50:155–172
- Leggat W, Hoegh-Guldberg O, Dove S, Yellowlees D (2007). Analysis of an EST library from the dinoflagellate (*Symbiodinium* sp.) symbiont of reef-building corals I. *J Phycol* 43:1010–1021
- Lesser MP (2006) Oxidative stress in marine environments: biochemistry and physiological ecology. *Annu Rev Physiol* 68:253–278
- Lesser MP, Farrell JH (2004) Exposure to solar radiation increases damage to both host tissues and algal symbionts of corals during thermal stress. *Coral Reefs* 23:367–377
- Levin RA, Beltran VH, Hill R, Kjelleberg S, McDougall D, Steinberg PD, van Oppen MJ (2016) Sex, scavengers, and chaperones: transcriptome secrets of divergent *Symbiodinium* thermal tolerances. *Mol Biol Evol* 33:2201–2215
- Lin S, Cheng S, Song B, Zhong X, Lin X, Li W, Li L, Zhang Y, Zhang H, Ji Z, Cai M (2015) The *Symbiodinium kawagutii* genome illuminates dinoflagellate gene expression and coral symbiosis. *Science* 350:691–694

- Mayfield AB, Hsiao Y-Y, Chen H-K, Chen C-S (2014) Rubisco expression in the dinoflagellate *Symbiodinium* sp. is influenced by both photoperiod and endosymbiotic lifestyle. *Mar Biotechnol* 16:1–14
- McGinley MP, Aschaffenburg MD, Pettay DT, Smith RT, LaJeunesse TC, Warner ME (2012) Transcriptional response of two core photosystem genes in *Symbiodinium* spp. exposed to thermal stress. *PLoS One* 7:e50439
- McGinty ES, Pieczonka J, Mydlarz LD (2012) Variations in reactive oxygen release and antioxidant activity in multiple *Symbiodinium* types in response to elevated temperature. *Microb Ecol* 64:1000–1007
- Miller AF (2012) Superoxide dismutases: ancient enzymes and new insights. *FEBS Lett* 586:585–595
- Oakley CA, Hopkinson BM, Schmidt GW (2014) Mitochondrial terminal alternative oxidase and its enhancement by thermal stress in the coral symbiont *Symbiodinium*. *Coral reefs* 33:543–552
- Parkinson JE, Baums IB (2014) The extended phenotypes of marine symbioses: ecological and evolutionary consequences of intraspecific genetic diversity in coral algal associations. *Front Microbiol* 5:445
- Parkinson JE, Coffroth MA, LaJeunesse TC (2015) New species of Clade B *Symbiodinium* (Dinophyceae) from the greater Caribbean belong to different functional guilds: *S. aenigmaticum* sp. nov., *S. antillogorgium* sp. nov., *S. endomadracis* sp. nov., and *S. pseudominutum* sp. nov. *J Phycol* 51:850–858
- Pochon X, Gates RD (2010) A new *Symbiodinium* clade (Dinophyceae) from soritid foraminifera in Hawai'i. *Mol Phylogenet Evol* 56:492–497
- Pochon X, Putnam HM, Gates RD (2014) Multi-gene analysis of *Symbiodinium* dinoflagellates: a perspective on rarity, symbiosis, and evolution. *PeerJ* 2:e394
- Ragni M, Airs RL, Hennige SJ, Suggett DJ, Warner ME, Geider RJ (2010) PSII photoinhibition and photorepair in *Symbiodinium* (Pyrrhophyta) differs between thermally tolerant and sensitive phylotypes. *Mar Ecol Prog Ser* 406:57–70
- Rhoads DM, Umbach AL, Subbaiah CC, Siedow JN (2006) Mitochondrial reactive oxygen species. Contribution to oxidative stress and interorganellar signaling. *Plant Physiol* 141:357–366
- Roberty S, Bailleul B, Berne N, Franck F, Cardol P (2014) PSI Mehler reaction is the main alternative photosynthetic electron pathway in *Symbiodinium* sp., symbiotic dinoflagellates of cnidarians. *New Phytol* 204:81–91
- Roberty S, Fransolet D, Cardol P, Plumier JC, Franck F (2015) Imbalance between oxygen photoreduction and antioxidant capacities in *Symbiodinium* cells exposed to combined heat and high light stress. *Coral Reefs* 34:1063–1073
- Roberty S, Furla P, Plumier JC (2016) Differential antioxidant response between two *Symbiodinium* species from contrasting environments. *Plant Cell Environ* 39:2713–2724
- Robison JD, Warner ME (2006) Differential impacts of photoacclimation and thermal stress on the photobiology of four different phylotypes of *Symbiodinium* (pyrrhophyta) 1. *J Phycol* 42:568–579
- Rodriguez IB, Lin S, Ho J, Ho TY (2016) Effects of trace metal concentrations on the growth of the coral endosymbiont *Symbiodinium kawagutii*. *Front Microbiol* 7:82
- Rosic NN, Pernice M, Rodriguez-Lanetty M, Hoegh-Guldberg O (2011) Validation of housekeeping genes for gene expression studies in *Symbiodinium* exposed to thermal and light stress. *Mar Biotechnol* 13:355–365
- Schrader M, Fahimi HD (2006) Peroxisomes and oxidative stress. *BBA Mol Cell Res* 1763:1755–1766
- Smith DJ, Suggett DJ, Baker NR (2005) Is photoinhibition of zooxanthellae photosynthesis the primary cause of thermal bleaching in corals? *Glob Change Biol* 11:1–11
- Sorek M, Yacobi YZ, Roopin M, Berman-Frank I, Levy O (2013) Photosynthetic circadian rhythmicity patterns of *Symbiodinium*, the coral endosymbiotic algae. *Proc R Soc Lond [Biol]* 280:20122942
- Suggett DJ, Warner ME, Smith DJ, Davey P, Hennige S, Baker NR (2008) Photosynthesis and production of hydrogen peroxide by *Symbiodinium* (pyrrhophyta) phylotypes with different thermal tolerances 1. *J Phycol* 44:948–956
- Suggett DJ, Goyen S, Evenhuis C, Szabó M, Pettay DT, Warner ME, Ralph PJ (2015) Functional diversity of photobiological traits within the genus *Symbiodinium* appears to be governed by the interaction of cell size with cladal designation. *New Phytol* 208:370–381
- Takahashi S, Whitney S, Itoh S, Maruyama T, Badger M (2008) Heat stress causes inhibition of the de novo synthesis of antenna proteins and photobleaching in cultured *Symbiodinium*. *Proc Natl Acad Sci* 105:4203–4208
- Tchernov D, Gorbunov MY, de Vargas C, Yadav SN, Milligan AJ, Häggblom M, Falkowski PG (2004) Membrane lipids of symbiotic algae are diagnostic of sensitivity to thermal bleaching in corals. *Proc Natl Acad Sci USA* 101:13531–13535
- Walker NJ (2002) A technique whose time has come. *Science* 296:557
- Warner ME, Suggett DJ (2016) The photobiology of *Symbiodinium* spp.: linking physiological diversity to the implications of stress and resilience. In: Dubinsky Z, Stefano G (eds) *The Cnidaria, past, present and future*. Springer International Publishing, Switzerland, pp 489–509
- Warner ME, Fitt WK, Schmidt GW (1996) The effects of elevated temperature on the photosynthetic efficiency of zooxanthellae in hospite from four different species of reef coral: a novel approach. *Plant Cell Environ* 19:291–299
- Warner ME, Fitt WK, Schmidt GW (1999) Damage to photosystem II in symbiotic dinoflagellates: a determinant of coral bleaching. *Proc Natl Acad Sci* 96:8007–8012
- Warner ME, LaJeunesse TC, Robison JD, Thur RM (2006) The ecological distribution and comparative photobiology of symbiotic dinoflagellates from reef corals in Belize: potential implications for coral bleaching. *Limnol Oceanogr* 51:1887–1897
- Wietheger A, Fisher PL, Gould KS, Davy SK (2015) Sensitivity to oxidative stress is not a definite predictor of thermal sensitivity in symbiotic dinoflagellates. *Mar Biol* 162:2067–2077
- Wolfe-Simon F, Starovoytov V, Reinfelder JR, Schofield O, Falkowski PG (2006) Localization and role of manganese superoxide dismutase in a marine diatom. *Plant Physiol* 142:1701–1709